Precambrian Phosphorites in the Bijawar Rocks of Hirapur-Bassia Areas, Sagar District, Madhya Pradesh, India[1,2]

D. M. Banerjee*, M. W. Y. Khan, Neeta Srivastava, and G. C. Saigal

Department of Geology, University of Delhi, Delhi, India

The Precambrian phosphorites of Bijawar Group of rocks show characteristics of a epicontinental sea with restricted and very shallow marine environment of formation along some shoals, which existed during the iron-rich Precambrian times. These phosphorite deposits located in the Hirapur-Bassia areas show extensive leaching of carbonate and phosphate minerals during episodes of weathering. X-ray diffraction studies indicated that carbonate-flourapatite is the major apatitic phase in these phosphorites while crandallite developed on the surface outcrops. There is a general tendency for the depletion of CO_2 in these apatites leading to formation of flourapatite. This CO_2 is an indicator of hidden weathering in the rocks. Major and trace element determinations of phosphorite have been used to indicate various correlation factors responsible for the concentration of elements in these Precambrian leached phosphorites.

* Present address:
Palaeoatmosphere Research Group
Air Chemistry Department
Max-Planck-Institut für Chemie
Postfach 3060
D-6500 Mainz
Federal Republic of Germany

INTRODUCTION

The Bijawar Group of rocks constitute a well defined, though poorly studied rock entity, and is named after the township of Bijawar, where they define the eastern Bijawar Basin. The name Bijawar was given to the early Precambrian sediments resting over the primordial Bundelkhand granite massif and underlying the Upper Proterozoic Vindhyan Group of sandstones (Medlicott, 1859). Mathur (1960) and Mathur and Mani (1978) carried out geological mapping of the type Bijawar basin and the stratigraphic succession of the area after these authors is given below:

VINDHYAN GROUP   SEMRI FORMATION
(Upper Proterozoic)

———————————————————— Unconformity ————————————————

                              Gangau Ferruginous Formation   Tillite and Shale
                                                             Ferruginous
                                                             conglomerate and
BIJAWAR GROUP   breccia
                              Bajna Dolomite
                              Amronia Quartzite
                              Dargawan Traps
                              Malhera Breccia

                    BUNDELKHAND GRANITE and GNEISSES

   Our present interest lies in the Gangau Ferruginous Formation of the above scheme which contains reddish-brown phosphorite in its lower parts, bordering the granitic rocks of Bundelkhand massif. In the Hirapur-Bassia areas, Bundelkhand granites are either directly overlain by Bajna Dolomite or come in direct contact of Gangau Ferruginous Formation containing conglomerates, breccia and shales (Fig. 2). There is no 'tillite' in the vicinity of the phosphorite horizon, but has been recorded in the adjacent regions (Mathur and Mani, 1978). Open synclinal and anticlinal structures are prominent in the shales and the Gangau Formation is locally bounded by a synformal structure in the Bassia area (Fig. 1). Some preliminary information about this deposit is contained in the review by Pant (1980). Similar phosphorites also occur at Sonrai in the Lalitpur district, west of Hirapur, where copper, lead-zinc and uranium minerals are intimately associated with the secondary phosphate horizons.

   Authors shared responsibilities for different tasks, viz. Banerjee for geological mapping, sampling, geological and geochemical interpretations, mineralogy, overall synthesis and writing, Khan for the major and trace element analyses by AAS and other techniques, and Srivastava and Saigal for X-ray diffraction studies.

PETROLOGICAL CHARACTERS

Since, only the underlying carbonates and the top phosphorites are of direct relevence to the present paper, the litho-characteristics of only these two rock types have been described. The fine grained Bajna Dolomites are of two types, namely: (a) brown ferruginous dolomite and (b) grey dolomitic limestone. The first type grades into overlying Gangau Formation. Their composition vary from cherty, shaly dolomite to pure dolomite rock. The Gangau Formation on the other hand are composed of ferruginous breccia, conglomerate and reddish brown slates and shales. The ferruginous sandstone and ferruginous shale occur as intercalations within the ferruginous conglomerate and breccia with abundant apatite grains in the groundmass. Based on the nature of occurrence in the area, four categories of phosphorites have been recognized:

Type I: Ferruginous, shaly, laminated phosphorite
Type II: Massively bedded, ferruginous phosphorite
Type III: Brecciated/Conglomeratic, ferruginous phosphorite
Type IV: Veins/Pore filling type, remobilized, secondary, crystalline apatitic, phosphorite.

   In Type-I phosphorite, microgranular apatite grains occur within the ferru-

GEOLOGICAL MAP OF HIRAPUR AREA
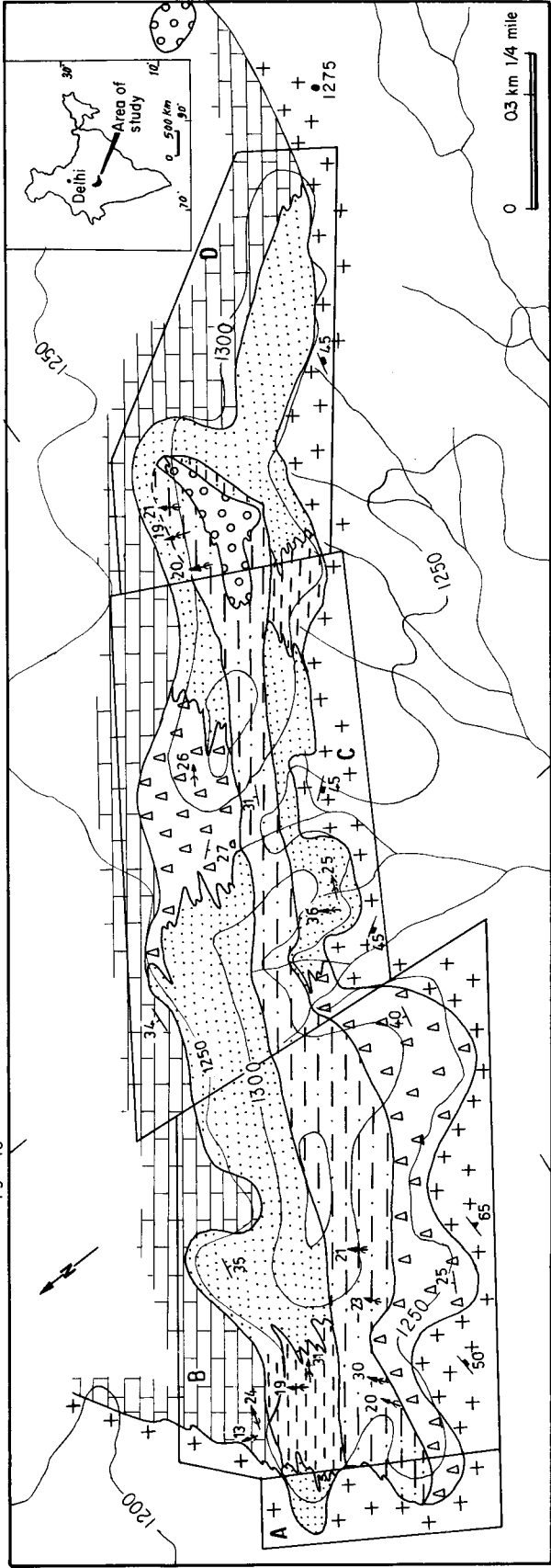
INDEX

Brecciated Phosphorite
Laminated Phosphorite
Massive Phosphorite

Gangau Formation

Dry Stream
Contour with value in feet
Exploration Block
Foliation
Dip of bed
Joint
Anticlinal fold axis
Synclinal fold axis

Shale
Bajna Dolomite
Quartzite
Bundel Khand Granite

Area of study
Delhi

Fig. 1. Lithological distribution map of Bassia phosphorite production area in Hirapur-Bassia sector. Location map in the inset
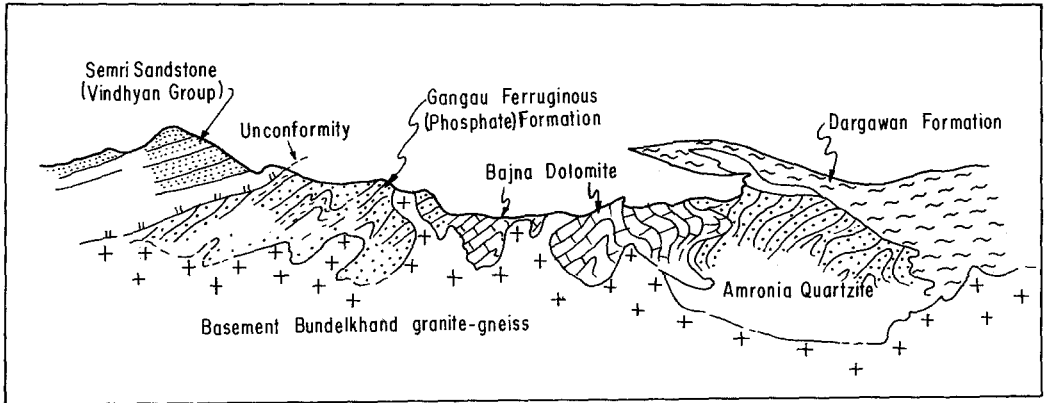
Fig. 2. Schematic/diagrammatic cross section across the phosphorite deposits in Hirapur-Bassia-Mardeora area. Scale approximate

ginous shaly matrix either as dispersed matter or as well developed microlaminations. Visual estimates of mica - clay mineral abundance in thin sections gives an inverse relationship with the quantity of apatite grains. Recrystallized coarse (0.02-0.15 mm) apatitic veins traverse through the shales (Fig. 3), mostly in a random manner or along secondary surfaces.

The Type-II phosphorites are massive, hard and compact, very fine grained, with thin laminations of coarse-grained quartz. Apatite is randomly distributed in the micaceous groundmass and occur as small crystallites (0.02-0.05 mm). Interstitial subhedral to anhedral elongated polycrystalline quartz (0.01-0.02 mm) show dissolution features on their margins. Subrounded to subangular fragments of ferruginous shaly phosphorite sometimes occur embedded in this type of ore, suggesting a later origin of this type of phosphorite. The void filling type of secondary apatite riddled with disseminated ferruginous matter occur with well defined rims of magnetite (Fig. 4). Such apatite are usually large (0.05-0.25 mm) and show successive growth layers. Pore filling episode shows the following stages of evolution:

(a) Apatite crystals growing outward with long axes normal to the confining

wall have ferruginous inclusions along successive layerings. Some of them show curved twin planes (Fig. 5). Possibly some of the ferruginous layers were pre-existing which were removed during dissolution process and precipitation of the apatites;

(b) Overgrowths of clear apatite on the pre-exisitng clouded apatite grains indicate authigenic precipitation;

(c) Precipitation of quartz in the remaining voids of the pore spaces;

(d) Iron oxide (magnetite/goethite) forming in the late stages of diagentic alterations.

The Type-III phosphorites contain ferruginous cement and occur in association of conglomeratic and brecciated quartzites. More or less equant apatite crystallites (0.01 mm) in a shaly groundmass contain profuse iron-oxide disseminations.

The Type-IV phosphorite occur as lateritic cover with well developed reniform surfaces. Large, perfectly crystalline prismatic apatite grains (0.05-0.25 mm) radiate into the voids and pores (Fig. 4). The microcrystalline groundmass is stained reddish brown by the secondary iron-oxides. A more detailed petrological description is given by Banerjee (1982).
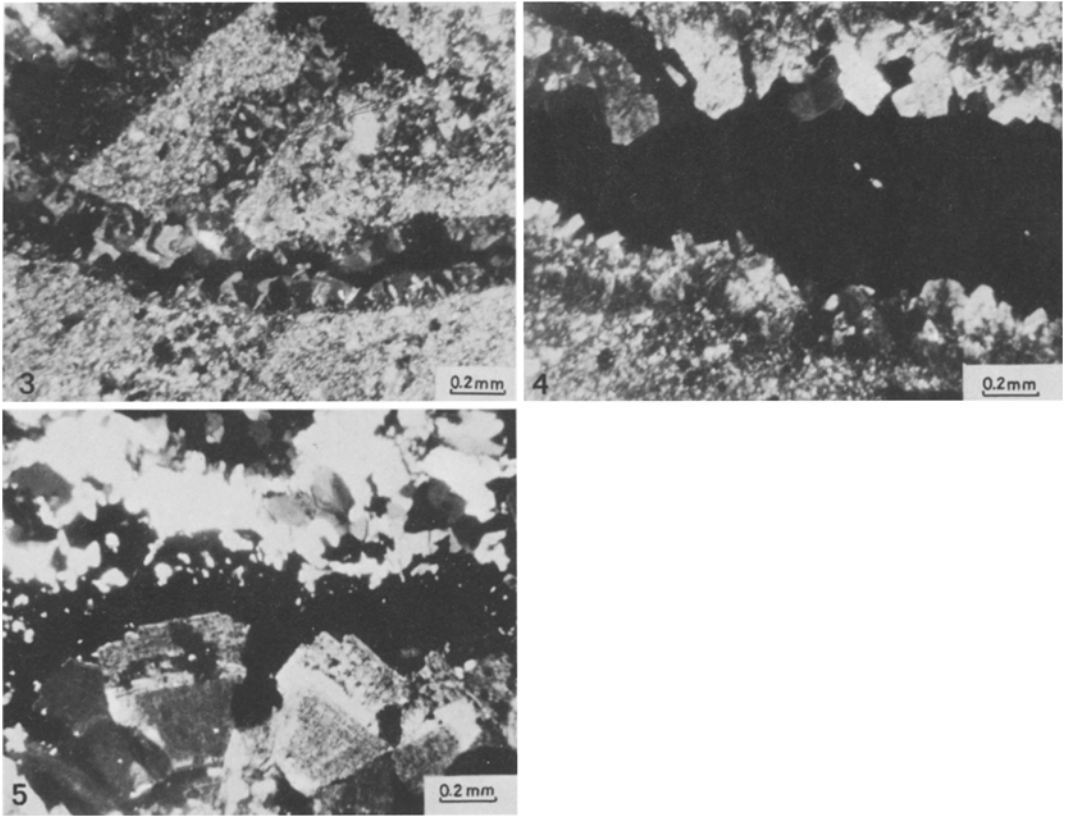
Fig. 3. Photomicrograph of Type-I phosphorite showing recrystallized coarse grained apatite crystals occurring within randomly oriented secondary veinlets in a predominantly areno-argillaceous groundmass. (X-nicols)

Fig. 4. Photomicrograph of void-filling type phosphorite with well developed apatite crystallites growing in size towards the open void spaces. Dark magnetite layers occur normal to the growth direction of the apatite crystallites. (X-nicols)

Fig. 5. Photomicrograph showing curved twin planes of apatite crystallites and their growth along the cavity margins. Secondary magnetite fills the remaining void spaces and also permeates into the twin planes of the apatite. (X-nicols)

MINERALOGY

Characteristic x-ray diffraction patterns shown in Fig. 6A and B reveal that carbonate-flourapatite is the major constituent, while quartz is the major gangue. There is, however, a general prevalence of carbonate-poor (CO_2: 0.10-2.85%) flourapatites. The diffraction pattern of the bulk samples, especially those from the top, weathered profiles, show positional shifts in the diffraction peaks from those known from an ideal carbonate-flourapatite and a number of secondary peaks remain sup-
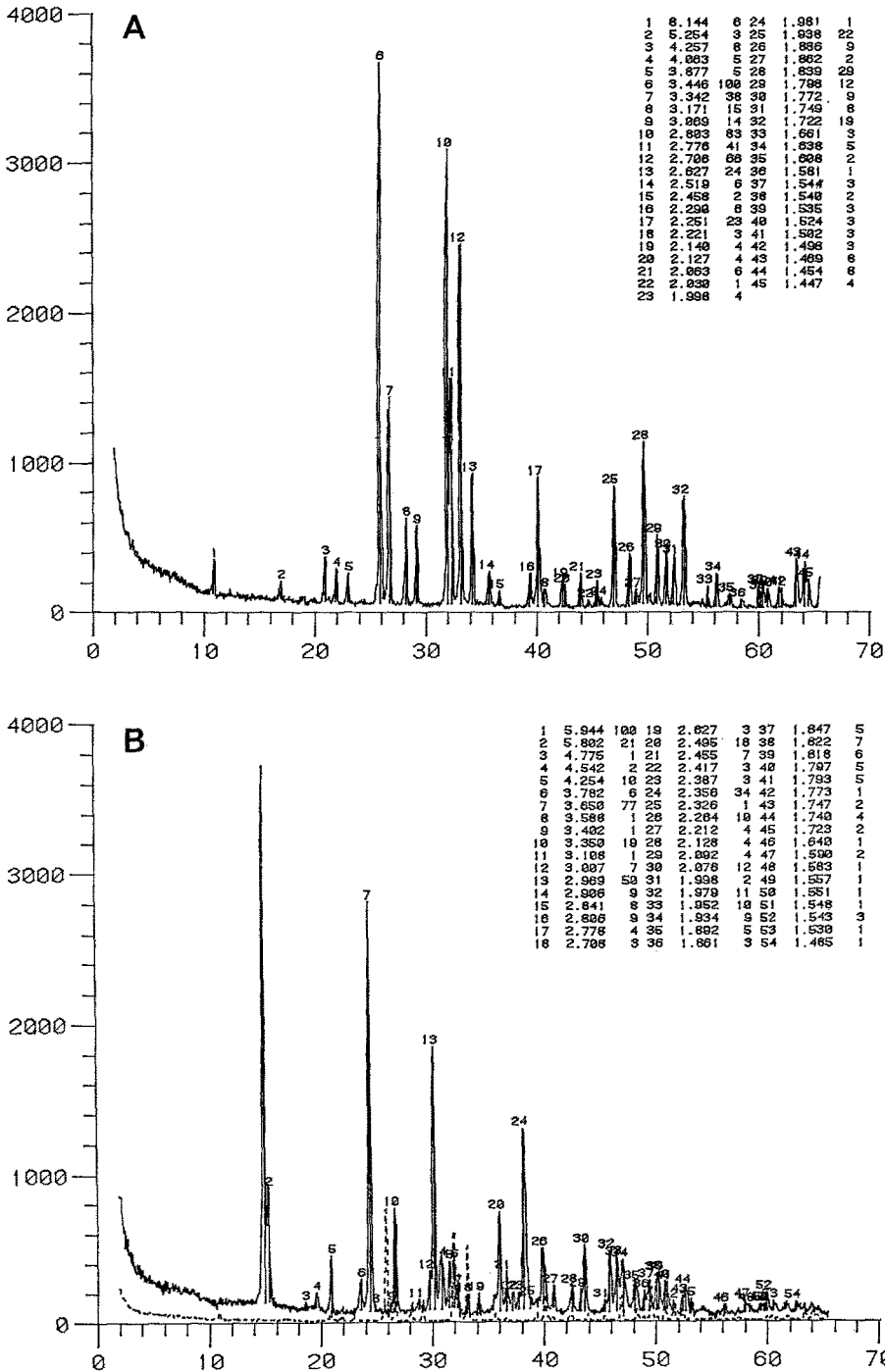
Fig. 6. A A typical X-ray diffractogram of bulk phosphorite showing prominent apatite peaks. B A X-ray diffractogram of phosphorite concentrate after apatite peaks are removed by computer stripping technique. The remnant peaks show the presence of crandallite

pressed due to overlapping by the pre-
dominant apatite peaks in most phos-
phorites. Using a computer programme,
all apatite peaks were stripped-off from
the diffraction patterns, which resulted
in the enhancement of the suppressed
peaks. The residual pattern (Fig. 6B)
is comparable to crandallite (ASTM
file no. 16-162) - an aluminous phos-
phate, which seem to have formed by
variable substitutions in the apatite
structure along the apatite → crandal-
ite → millisite weathering series.
The lattice parameters were calculated
from the observed diffraction patterns
and by referring to hexagonal axes with
the equation:

$$a^O = \sqrt{1.3333 \ d^2 \ (h^2 + k^2 + hk)}$$

for (210), (310), (320) and (410) planes
and c^O = 1. d for (004) and (002) planes.
Lattice dimensions of the apatite (car-
bonate-flourapatite) crystallite vary be-
tween 9.29 Å - 9.379 Å for a_O and
6.880 Å for c_O, whereas for crandallite
a_O is recorded as 7.83 Å and c_O as
9.67 Å. CO_2 was determined by the
peak-pair method of Gulbrandsen (1970),
which varies from 0.10 to 2.85%.

The summary of axes in the unit cell
of apatite shows no significant differ-
ence between the mean length in the
unleached and weathered phosphorites,
which varies from 9.29 Å in weathered
phosphorites, to 9.37 Å in massive un-
leached phosphorites. CO_2-a_O plots
show a wide scatter and random corre-
lation suggesting extensive leaching dur-
ing weathering.

CHEMICAL COMPOSITION

Spectrophotometric determination of
major elements were carried out using
the U.S. Bureau of Analytical Standards
BCR_1 and GSP_1 and B.A.S. Standards
(U.K.) the Thomas Phosphate 31-A.
Trace elements were determined by
atomic absorption and x-ray floures-
cence techniques. Table 1 depicts the

major elements and recalculated molar
percentages of average Hirapur apa-
tites. The observed charge imbalanc-
ing is due to the unaccounted flourine
content which was not determined dur-
ing the present work. Higher concen-
tration of $P_2 O_5$ is noticed in the
weathered phosphorites (Type IV). Sili-
ca show gradual decrease with increas-
ing $P_2 O_5$, while Ca increases simul-
taneously. However, the total Si values
have not been considered for any inter-
pretations, whose distribution in the
rock is controlled by both diagenetic
and secondary quartz. Similarly, the
primary association of iron with phos-
phorite is not established with certaini-
ty. Na content is fairly high compared
to any known phosphorite types from
India. All trace elements show low con-
centrations with few exceptions. The
intercorrelation of elements define three
major associations such as: (1) apatitic
phosphorite, (2) ferruginous-clayey
phosphorite and (3) weathered (leached)
aluminous phosphorite. Each element
association reflects a grouping of ele-
ments: (a) structurally substituted in
major mineral apatite, (b) adsorbed
onto the mineral surface or (c) exist-
ing as discrete minerals derived from
apatite by weathering. Most elements
actually exist in more than one associ-
ation. The element distribution pattern
in the apatite structure indicate a posi-
tive correlation of CaO and $P_2 O_5$
(Fig. 7A). To establish the inter-element
relationships, linear or otherwise, all
the samples with variable $P_2 O_5$ con-
tents have been plotted. The major ele-
ment regression plots of CaO - $P_2 O_5$,
$P_2 O_5$ - CO_2 and CaO - Na_2O are given
in Fig. 7A-C. Since, the range of val-
ues of minor elements are of less sig-
nificance, the comparison of major ele-
ments has been deemed to be possible
between different petrological and chem-
ical types. Comparison of less-weather-
ed phosphorites with the weathered ones
and variations in the composition of
their contained carbonate-apatite as re-
flected by the normalised structural
concentration values can be taken as
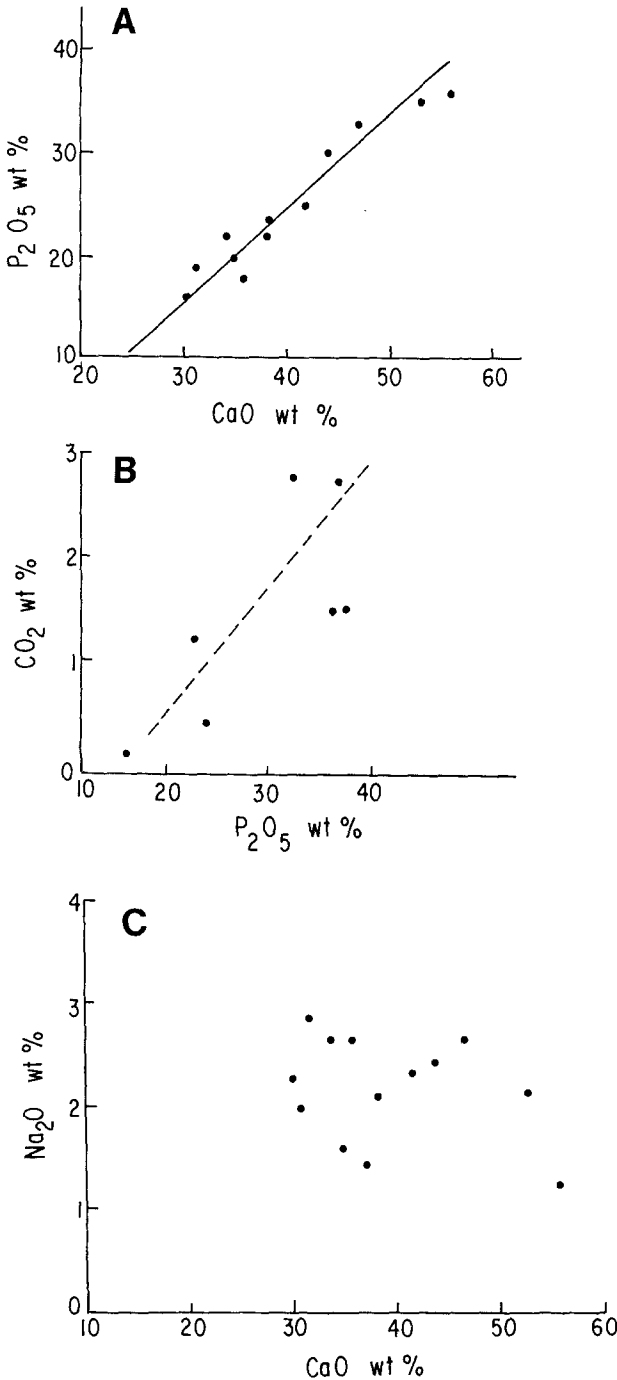the measure of the chemical ingradients

Fig. 7A-C. Regression plots showing:
A Positive correlation of CaO and
$\overline{P}_2O_5$. B Crude linear relationship of
P_2O_5 and CO_2. C Negative correla-
tion of CaO and Na_2O

of the depositional waters at the time of the phosphorite formation. Those elements which indicate negative correlation e. g. most of the plots of Na_2O with respect of CaO suggest that only very small part of Na_2O has substituted in the apatite structure, while the rest of it occurs in association of other minerals. This random distribution pattern also reflects varying degree of weathering at different locations. There is consistent decrease in the overall trace-element concentrations in the more weathered phosphorites except for Mn, which tend to be fairly high in weathered profiles (Table 2). Such a distribution pattern of trace elements indirectly suggest a positive correlation of various elements with CaO and P_2O_5 - the essential constituents of the carbonate-flourapatite.   Trace elements like U and Th show positive interelement correlation along the entire profile (Fig. 8) from weathered to least weathered phosphorites. The CaO/ Th, U correlation is represented by a curve which shows that the increase of U and Th with gradual decrease of CaO is a product of apatite-calcite leaching/ weathering near to the surface. Since the depth of weathering is not uniform, the distribution pattern of U and Th with respect to CaO and P_2 O_5 also varies in the same proportion. Therefore, it can be assumed that both U and Th have no strong correlation either with the apatites nor with the crandallites, but have been concentrated in the rocks as a result of leaching. Figure 8 depicts the absolute abundance of U with progressive leaching within the deposit. The ratio of Th/U varies from 0. 23 to 0. 42 with a mean of 0. 32 and this is considered significantly higher that the worldwide average of 0. 10 (Wedepohl, 1969). It is however possible that Th may have some crude affinity for the crandallite in the shaly phosphatic horizons. This type of relationship can be interpreted to be due to variability in the depths of leaching, and thus, suggest that most of U and Th in these rocks have formed by the process of secondary enrichment. CO_2
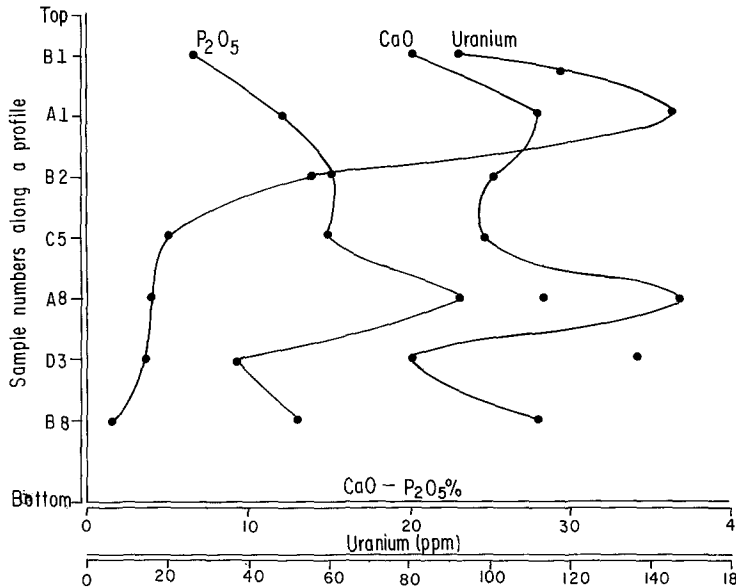
Fig. 8. Graphic presentation of absolute abundance of uranium with progressive leaching within the phosphorite deposit of Hirapur-Bassia area
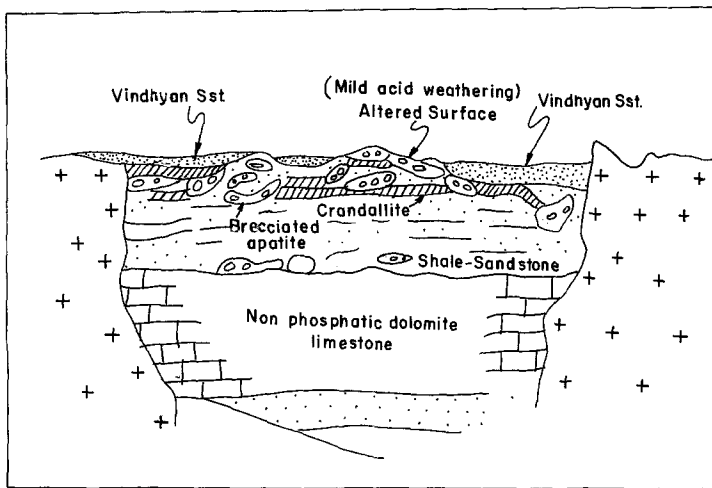
Fig. 9. Schematic diagram of the distribution pattern of phosphorite in a weathering/leaching profile at Hirapur-Bassia area (scale arbitrary)

shows a weak and crude linear relationship (Fig. 7B) with P_2O_5 in most apatites, but in more weathered rocks the CO_2 content is higher, possibly due to secondary vein-filling calcites, and in this, the plots deviate significantly from linearity. This near random correlation also indicates variable leaching.

DISCUSSION

The dolomitic limestone bottom at Bassia is abruptly followed by sandy apatitic phosphorite and then by sandy clayey ferruginous phosphorite layers, each one of these show transition into other phosphorite types depending upon

degree and intensity of weathering (Fig. 9) leaching, collapse and recementation. The bottom-most part of the phosphorite unit appears to have formed by the phosphatization of carbonates, although the sharp boundaries between the two does not convincingly prove such an interpretation.

The chemistry shows that these carbonate-flourapatites are poor in CO_2 content. In more weathered phosphorites, mineral phases of crandallite are more prominent, inspite of the presence of a dominant apatite phase. In carbonate-flourapatites, 4% CO_2 is considered normal concentration, consequently the low CO_2 values (Table 1) of the Hirapur-Bassia apatites is due to the processes of decarbonation, caused by the dissolution and reprecipitation. The early illite-montmorillonite assemblage seem to have transformed into muscovite, which accounts for most of the K and Al present in these phosphorites. A part of K seem to have been derived from the potassic minerals of the cratonic mass of Bundelkhand granitic complex which also provided land derived phosphorus through weathering of the terrestrial cover. As mentioned earlier, trace element content is low in the shaly and lateritic phosphorites compared to massive bedded phosphorites. Most trace elements seem to have leached out of the system during prolonged episodes of weathering and leaching. The irregular distribution of crandallite is also due to differential weathering of shaly apatitic phosphorites. The carbonate flourapatite → crandallite (Ca) transformation in these phosphorites appear to be in their early stages, compared to phosphorites of the Sonrai area of the western Bijawar basin, where minerals of more advanced weathering stages → millisite → wavellite are also recorded. It is possible that the paragenetic sequence would have been the same as those identified in the Sonrai area, West Senegal, parts of Florida, Rumjungle area in Australia and parts of USSR, provided the Hirapur-Bassia basin was not protected from the onslaught of weathering for a considerable time after they were lithified and uplifted. It is worth recalling that Mathur and Mani (1978) recorded glacial tillites in the adjacent non-phosphatic area, apparently overriding the Gangau Formation and possibly marking the unconformity over which the Lower Vindhyan sandstones were deposited. It can therefore be visualized that towards the closing phases of Gangau sedimentation, warmer climates changed to cooler ones which helped in protecting the basic carbonate-flourapatitic character of the Hirapur-Bassia phosphorite. It is therefore possible that the weathering was not prominent during the Precambrian times but was initiated vigourously during the subsequent periods. During the last phases of evolution of Bijawar rocks, land conditions prevailed with local fluvial influences and groundwater circulation through the exposed rock masses. The ferruginous crust, so common in such environments, were formed locally, but the sandstone-shales developed more extensive ferruginous coatings which also filled the intergranular spaces. This phase is associated with recrystallised alumino-calcic phosphatic cement which occur as vugs and cavity fillings within the alumino-phosphate rich phosphorites. There is gradual decrease in the detrital quartz content from the bottom to the top, and cement is more prominent in the surficial shales and phosphorites. In such places where the leaching was more intense, it induced numerous dissolution features leading to the formation of pseudo-breccia by the removal of cement, collapse and recementation by circulating groundwater containing dissolved iron.

It is significant to note that various mineral transformations noted above have not disrupted any of the primary stratification or the microtextures, which suggest that these transformation reactions were apparently isovolumetric due to leaching by permanent groundwater which received its supply through

Table 1. Chemical composition and recalculated mole percentage of average phosphorite of Hirapur-Bassia area

Phosphorite type	Shaly laminated phosphorite		Massively bedded ferruginous phosphorite				Brecciated ferruginous phosphorite			Vein/Pore filling remobilized type phosphorite		
Sample No.	B-1	C-2	D-6	C-3	D-10	D-(Ave)	B-4	B-9	D-3	A-4	SM	SC
Composition in wt.%												
SiO2	31.04	26.07	27.79	28.37	27.30	20.22	23.11	2.75	10.56	4.37	4.65	1.38
Al2O3	6.95	5.74	6.09	0.18	1.83	1.19	—	1.79	0.67	1.35	—	0.54
Fe2O3	9.12	1.27	0.99	4.35	5.75	1.28	27.22	0.56	6.78	1.84	0.96	0.75
Na2O	2.23	2.63	1.56	0.20	1.93	2.30	1.41	—	2.45	2.60	2.08	1.14
K2O	2.75	2.53	2.27	0.26	1.40	1.34	0.13	0.07	0.45	1.33	0.42	0.08
CaO	30.04	34.64	35.25	38.86	31.06	42.25	38.02	36.04	44.47	47.66	53.27	56.05
MgO	1.33	0.87	0.80	0.51	0.62	0.95	0.55	0.56	0.58	0.43	0.15	0.09
P2O5	16.57	22.48	20.19	23.90	19.67	25.30	22.23	18.06	30.11	33.21	35.14	36.98
H2O-	0.003	0.003	0.004	0.003	0.001	0.003	0.005	0.004	0.003	0.003	0.36	0.004
L.O.I	1.30	0.80	1.20	1.05	1.06	1.05	1.12	0.97	1.41	1.80	3.42	3.21
CO2*	0.10	1.25	nil	0.45	2.50	nil	nil	nil	2.85	nil	1.60	1.60
Recalc. moles in %												
CaO	8.282	8.600	8.996	8.968	8.771	8.518	7.895	8.669	8.947	9.000	9.306	9.637
MgO	0.606	0.283	0.2834	0.163	0.242	0.2761	1.585	0.186	0.161	0.112	0.036	0.021
Na2O	1.111	1.117	0.7200	0.868	0.983	0.8719	0.524	0.144	0.891	0.887	0.657	0.341
P2O5	5.999	5.506	5.999	5.823	4.979	5.999	5.999	6.000	5.205	5.999	5.590	5.609
CO2	0.005	0.493	—	0.176	1.020	—	—	—	0.794	—	0.409	0.390
Charges Total cations	+18.887	+18.884	+19.279	+19.130	+19.013	+19.127	+19.474	+19.998	+19.108	+19.112	+19.341	+19.657
Total anions	-17.998	-17.506	-17.997	-17.821	-16.978	-17.997	-17.997	-18.000	-17.205	-17.997	-17.589	-17.608
Charge imbalance	0.885	01.338	01.282	01.309	2.145	01.130	01.477	01.998	1.903	01.115	01.751	2.048

* By X-ray peak-pair method of Gulbrandsen (1970)

Table 2. Trace element concentration in phosphorite

Sample No. →		B-1	B4/H1	D6/B2	C2/C5	A4/A8	D10/D3	C3/B8	D(Ave)	B-9	SM	SC
Locality →		Mardeora surface	Hirapur surface	Bassia surface	Bassia pit	Bassia pit	Bassia pit bottom	Bassia pit bottom		Bassia surface	Bassia surface	
Phosphorite Type →		I	III	I	I	IV	II	II	II	III	IV	IV
	1 U	130	120	—	20	20	10	10	—	—	—	—
	2 U	122	174	56.4	20	166.1	15.2	6.35	—	—	—	17
	3 Th	29	38	16	7.4	6.2	6.0	4.2	—	—	—	3
	4 Th/U	0.23	0.21	0.28		0.38	0.39	0.42	—	—	—	0.17
	5 Zn	128	125	475	1125	475	175	275	16501	300	200	875
	6 Cu	105	155	125	275	265	170	180	390	190	—	63
	7 Mn	125	325	140	135	375	142	50	425	5900	—	89
	8 Cr	120	—	0	85	575	300	4050	290	100	—	53
	9 Co	175	120	170	140	165	120	170	120	140	—	—
	10 Ag	50	25	75	24	25	12	60	25	150	—	—
	11 Ni	445	320	335	260	660	360	1550	280	375	—	20
	12 Cd	382	160	375	235	325	130	245	240	125	127	235
	13 Ba	—	58.4	—	—	39	100	72	—	—	—	—
	14 Ga	—	—	—	—	—	—	2	—	—	—	—
	15 Pb	—	—	—	—	—	—	14	—	—	—	13
	16 Sr	—	—	—	—	—	—	21	—	—	—	70
	17 V	—	—	—	—	—	—	15	—	—	—	22
	18 Y	—	—	—	—	—	—	14	—	—	—	21
	19 Zr	—	—	—	—	—	—	22	—	—	—	17

(Trace elements ← Trace elements →)

Samples B-1 to C-3 along a vertical profile.
1. Analyst: Dr. P.K. Bhargava/Dr. P.K. Cheria, Atomic Mineral Div., New Delhi.
2. Analyst: H.T. Millard Jr., R.B. Vaughn, S.W. Laster, and B.A. Keaton at USGS in Denver.
3. Thorium values are listed as "less than" the values shown.
5-12: Analysis by A.A.S. at Delhi University.
13-19: Analysis by X.R.F. at University of McQuarie and University of Keele.

the wet tropical rainfall, a condition that could very well be imagined to have existed in the central part of India where the Upper Bijawars are now exposed, at least from the Tertiary times, if not earlier.

The intensity of weathering is dependent on the mineral association and the most common effect is the loss of CO_2 in the carbonate flourapatite structure. As long as the carbonate is present in the rock it protects the associated apatite, halting the mineral transformation beyond the flourapatite stage (Lucas et al., 1980). Therefore, the apatites like those of Hirapur-Bassia area with low CO_2 contents could be safely interpreted to have evolved through the processes of weathering. With prolonged period of weathering, when carbonate was almost completely leached out, other associated minerals were attacked which released additional cations like Al and Fe. In the argillaceous host rocks, these released cations combined with available phosphates and formed crandallite, while in the alumina-poor detrital rocks, flourapatite remained the dominant phase and developed magnetite-goethite coatings. That iron was not readily available at the time of early phosphate sedimentation, is evident from the fact that no iron-phosphate has formed in the sequence. However, in the void-filling type remobilized and recrystallized phosphorites, it seems that some of these voids and fissures were occupied by ferruginous laminations which have been systematically leached and isovolumetrically replaced by crystalline apatite grains, growing from the margins towards the centre of the void spaces (Fig. 4). Such features suggest that small quantity of iron was possibly introduced into the system subsequent to primary phosphate sedimentation, possibly at late diagenetic stages, on the sediment-water interface and was subsequently leached out during early stages of weathering. Widespread ferruginous coatings of all the rocks in the area is due to region-al ferruginization process, which seem to have accompanied the regional silicification as the last stages of the geological activity in the region. It is also possible that some Fe was introduced in the sediments through epigenetic processes.

To summarize, the phosphorites of Hirapur-Bassia originated along restricted shoals in littoral basins of the intracratonic sea which fringed the margins of the Bundelkhand granitic craton. The shallow nature of the basin has been interpreted on the basis of occassional rippled sandy surfaces, current cross-laminations, horizontal and wavy laminations in the silty layers and primary parallel laminations and raindrop-imprints on the ferruginous shales. The environment was highly oxidizing, as evident from the abundance of hydrated and non-hydrated iron oxides, inspite of the fact that the basin had a restricted circulation. This also explains an observed fact that the organic matter contribution to the phosphate precipitation was negligible and the water depth of the sedimentation basin was extremely shallow, with occassional subaerial exposures. It is possible, such a shallow oxidizing basin was also responsible for higher concentration of Na in the phosphate rocks.

REFERENCES

Banerjee, D. M.: Lithotectonic, phosphate mineralization and regional correlation of Bijawar Group of Rocks in the Central India: In Geology of the Vindhyachal, Valdiya, K. S. (ed.) p. 26-39, Hindustan Pub. Corp. Delhi (1982)

Gulbrandsen, R. A.: Relation of carbon dioxide content of apatite of phosphorite formation to the regional facies: The Mountain Geologist. 8, 81-84 (1970)

Lucas, J., Flicoteaux, R., Nathan, Y., Prevot, L., Shahar, Y.: Different aspects of phosphorite weathering. S. E. P. M. Spl. Pub. No. 29, 41-51 (1980)

Mathur, S. M.: A note on the Bijawar Series in the eastern part of the type area, Chattarpur area, M. P. Rec. Geol. Surv. India 86, 539-544 (1960)

Mathur, S. M., Mani, G.: Geology of the Bijawar Group in the type area, M. P.: Proc. Symp. on Purana Formations of Peninsular India, Univ. of Sagar, Saugar, M. P. 313-320 (1978)

Medlicott, H. B.: On the Vindhyan rocks and their associates in the Bundelkhand. Mem. Geol. Surv. India 2, 1-95 (1959)

Pant, A.: Resource status of rocks phosphate deposits in India and areas of future potential: Proc. Fertilizer Raw Material Resources Workshop, East-West Center, Honolulu. Sheldon, R. P., Burnett, W. C. (eds.) 331-357 (1980)

Wedepohl, K. H.: Handbook of Geochemistry. New York: Springer, Berlin, Heidelberg, New York (1969)

Dr. D. M. Banerjee
Dr. M. W. Y. Khan
Miss. Neeta Srivastava and
Mr. G. C. Saigal
Department of Geology
University of Delhi
Delhi-110007
India